NUMERICAL ANALYSIS AND OPTIMIZATION OF MIXERS

Jônathas Assunção S. N. de Castro, jonathassun@yahoo.com.br
Taygoara Felamino de Oliveira, taygoara@unb.br
Universidade de Brasília, Campus Universitário Darcy Ribeiro, Brasília – DF, CEP 70910-900

Carlos Humberto Llanos Quintero, llanos@unb.br
Universidade de Brasília, Campus Universitário Darcy Ribeiro, Brasília – DF, CEP 70910-900

Abstract. *The purpose of this paper is to present numerical analysis of the CNG-air mixers and propose its geometric optimization. The mixer is the section where mixing between air and fuel occurs. This section is associated with loss of pressure energy, increasing the emission of pollutants and the loss of power in a combustion engine. This work aims the development of a mixer with lower pressure drop and more homogeneous mixture. The flow inside a conventional mixer is evaluated through a numerical methodology and its comparison with analytical and experimental results. The diffusion rate of the CNG and air molecules increases with the Reynolds number, however, in the prototype tested the quality of the mixture, i.e., its homogeneity independs of the flow Reynolds, being dependent only of the geometry of the mix section.*

Keywords*: OpenFOAM, mixer, orifice plate, turbulence, compressed natural gas (CNG).*

1. INTRODUCTION

Natural gas was brought to the center of the current debate on the issues of energy, environment and climate. One of his strengths that provided its leading position is the lower emissions of carbon dioxide per energy produced than other fossil fuels. The burning of CNG – compressed natural gas, is cleaner and more efficient, allowing therefore its penetration in various markets, including domestic and commercial heating, industrial processes and electricity.

In a recent study of MIT – Massachusetts Institute of Technology, can be noticed that natural gas is still slightly used in the automotive industry. Hence, there is a possibility of expanding its use as a fossil fuel in automotive vehicles mainly due to the fact of reducing by about 25% the greenhouse gas emission. However, one factor that reduces its use in this market is the increase of the initial costs of the vehicles that use natural gas as fuel, mainly the storage cost of the CNG on board (MIT, 2010).

The use of CNG in automotive vehicles requires the installation of a conversion kit. One of the components of the third generation kits is the mixer. This component is a geometrical section where the mixing between air and CNG occurs. The purpose of the mixer is to provide a homogeneous mixture of the fluids to the engine cylinders with the pressure drop as small as possible. However, the homogenization of the mixture occurs across a physical restriction to the flow on its admission, what generates the loss of engine power, increases the fuel consumption and increases the emission of pollutants (Castro, 2008).

In view of these problems and the lack of specific studies on the subject in the literature, it is proposed to analyze the mixing section CNG-air through a computational analysis of turbulent flows of the fuels. The overall motivation is to seek a geometrical restriction which improves the mixture homogeneity of CNG-air and decreases the loss of pressure energy, thus providing greater efficiency and less emission of pollutants by the engine adapted to the use of CNG.

In this context, the specific objectives are: (i) validate the numerical results obtained through the OpenFOAM® computational package by comparisons with analytical and experimental results of a machined prototype; (ii) characterize the pressure loss of the prototype and analyze the influence of the Reynolds number on the loss of pressure energy; (iii) characterize the mixture in the prototype through the diffusion of a passive scalar in the flow and analyze the influence of Reynolds number on the homogeneity of mixture; and (iv) conclude about the factors that affect the homogeneity of the mixture in mixers.

2. BIBLIOGRAPHICAL REVIEW

The geometrical section of the prototype used in the experiments is similar to flowmeters called orifice plate. The orifice plate is a load loss device which blocks the flow and causes a pressure drop. This pressure drop is a measure of the flow. The orifice plate follows the Bernoulli obstruction theory, which can be physically characterized by visualization of Fig. 1.

The flow in the duct diameter D_1 is forced through an obstruction diameter D_0. The index β of the device is a key parameter calculated as the ratio between the diameters D_0 and D_1. Also important, the discharge coefficient (C_d) is the dimensionless parameter which enables calculation of the fluid flow (Q) through the orifice plate by Eq. 1.

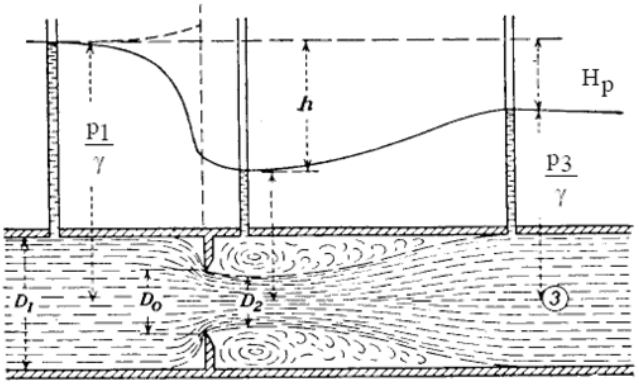

Figure 1: Physical characterization of an orifice plate.

$$Q = C_d \times A_0 \times \sqrt{\frac{2\Delta p/\rho}{1-\beta^4}} \quad (1)$$

The orifice plate can be used with β values between 0.2 and 0.8, taking the precaution that the smallest diameter don't be lower than 12.5 mm and that the Reynolds number of the flow at entry be within the range from 10^4 to10^7.

According to Fox, the widespread use of orifice plates in the flow measurement is due to the fact that it has a simple geometry, low cost and easy installation and replacement. Its main disadvantages are its limited capacity and high permanent pressure loss downstream of the measuring element (Fox, 2001).

Empirical values allow calculation of the analytic discharge coefficient through adjustments of the dimensionless curves that allow the establishment of the correlation equations for calculating the flow and / or pressure drop developed by the ISO – International Organization for Standardization (White, 2002). The Eq. 2 and Eq. 3 show the basic form of an analytical curve fitting allows calculation of coefficient of discharge of an orifice plate.

$$C_d = f(\beta) + 91{,}71\beta^2 Re^{-0.75} + \frac{0{,}09\beta^4}{1-\beta^4} F_1 - 0{,}0337\beta^3 F_2 \quad (2)$$

$$f(\beta) = 0{,}5959 + 0{,}0312\beta^{2{,}1} - 0{,}184\beta^8 \quad (3)$$

In Eq. 2 and Eq. 3, the correlation factors F_1 and F_2 depend on the position of the sockets, and, if taken with an equivalent distance D upstream and 0.5D downstream, , F_1 = 0,4333 and F_2=0.

By the computational fluid dynamics (CFD) techniques, the fundamental causes of the phenomena of turbulence are resolved and simulated using classical Transport Equation combined with turbulence models, and solvable through computational resources and sophisticated numerical methods (Launder and Spalding, 1972; Patankar and Spalding, 1972; Malhotra et al, 1994; Averous and Fuents, 1997; Cullivan et al, 2003).

3. MATERIALS AND METHODS

The results obtained in this work evolve starting from the numerical code validation. At first, it was compared the computational and theoretical results of the discharge coefficient of a pattern orifice plate. The equations described previously were used to obtain the theoretical C_d. In this stage was also evaluated the physical similarity of the flow downstream of the orifice plate obtained by numerical simulation.

Following validation, a prototype was built to evaluate the experimental pressure drop. A computational model of the prototype was processed for comparison of numerical results with experimental results and with the theoretical solutions.

Thirdly, computational solutions were obtained to characterize the diffusion of a passive scalar in the prototype tested as well as in an alternative geometry to conclude about the factors that influence the homogeneity of the mixture.

3.1 Numerical Formulation

The software used to process the simulations was the OpenFOAM®, an open source computational package based on the finite volume method. The geometric modeling and mesh generation computing was performed in Salome Meca® software, which is also an open source software that provides a generic environment for pre-processing and post-processing of numerical simulations. For data processing and image acquisition we used the Paraview® open source software.

In all simulated cases the fluid used was air (ν = 1,5x10-5 m²/s). We simulated three-dimensional incompressible and isothermal flow. It was adopted the following boundary conditions to process the simulations: at the inlet we established an axial velocity profile of the flow associated with a null pressure gradient; at the outlet we adopted the atmospheric pressure; at the walls we adopted a null velocity and modeling through the classical logarithmic law of wall (Munson, 2002).

The numerical simulations were processed in a steady state of a monophasic flow. The turbulent flow was solved through the κ-ε turbulence model and the average Reynolds equation (RANS). We used the SIMPLE numerical scheme for resolving the pressure-velocity coupling combined with an upwind interpolation scheme of the numerical code. In order to ensure the stability and the convergence of the numerical solution we used a convergence criterion of the order of 10^{-6} and relaxation factors of 0.3 for the pressure (Jones and Lauder, 1972).

To achieve the initial goal of validating the computational model, we simulated a geometrical section of an orifice plate with a diameters ratio (β) of 0,5 with D1 = 100 millimeters. The total length of the orifice plate is 1.500 millimeters and the Reynolds number of the flow at the inlet is 10.000. The mesh of Fig. 2 allows us to observe the presence of unstructured tetrahedral volumes. There are approximately 460.000 control volumes in the mesh generated by Salome Meca® software.

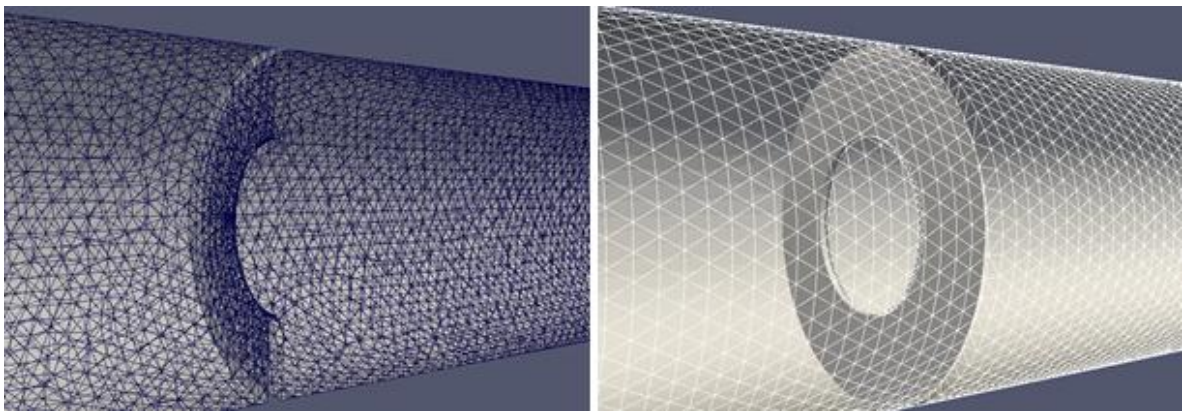

Figure 2: Tetrahedral mesh.

In a second step, seven computational simulations with different Reynolds numbers were processed with the geometry of the prototype to perform the necessary comparisons with experimental results of the flow bench. Each simulation was processed through 2.000 iterations, with approximately 150.000 volumes and 30.000 nodes. For this mesh, each simulation lasted about 10 hours.

The Reynolds numbers of the simulations were similar to the values used during the tests on the flow bench, as the table below:

Table 1: Reynolds numbers of the simulations.

Case	Case 1	Case 2	Case 3	Case 4	Case 5	Case 6	Case 7
U (m/s)	24,27	23,51	22,55	21,72	20,96	19,93	14,62
Reynolds	69.574	67.395	64.395	62.264	60.085	57.132	41.910

3.2 Experimental Methodology

A simplified prototype of a conventional mixer was built for the tests on the flow bench MOTORPOWER 200. Figure 3 illustrates the machined prototype, and the Table 2 shows its dimensions.

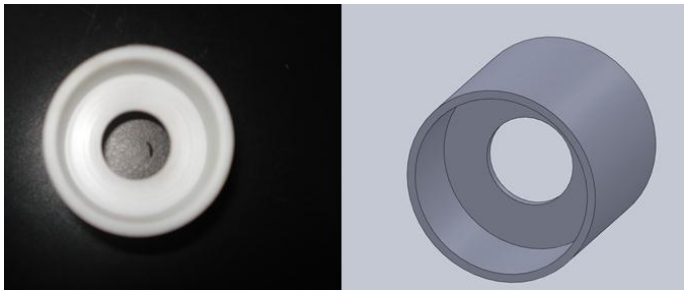

Figure 3: Machined prototype tested on the flow bench.

Table 2: Geometrical characteristics of the prototype.

Mixer diameter	43,0 mm
Ring restriction diameter	21,5 mm
Mixer length	40,0 mm

4. RESULTS AND DISCUSSION

4.1 Numerical Validation

The principal qualitative results obtained can be seen in Fig. 4, illustrating the *vena contracta*, the region of recirculation after the geometric obstruction, and the end of the flow separation, which follows the pattern shown in the theoretical approach of the orifice plate. It shows a good correlation between the qualitative results obtained by processing the simulation with the physical structures observed in literature.

It is observed the detachment of the flow in the region downstream of the obstruction, causing a recirculation zone or 'dead zone', with low pressure. Also, there is a region following the restriction where the flow may be further narrow, through a *vena contracta* of diameter $D_2 < D_0$. It is also clear that after the *vena contracta* there is a recovery load region.

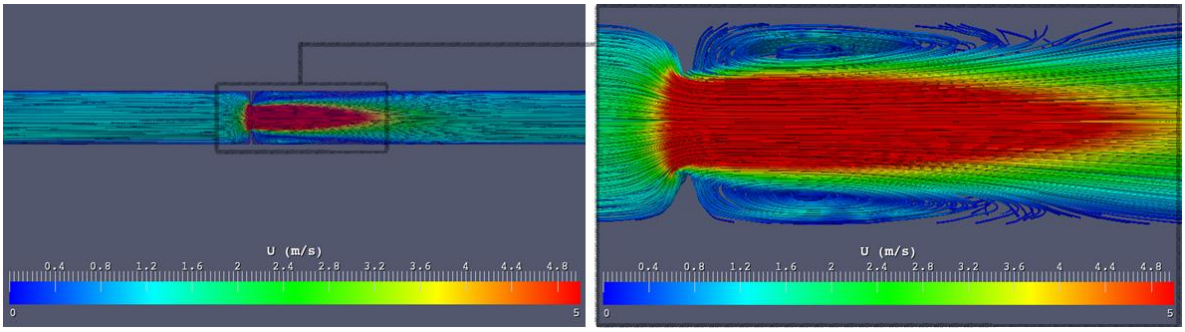

Figure 4: Visualization of the *vena contracta* in the orifice plate.

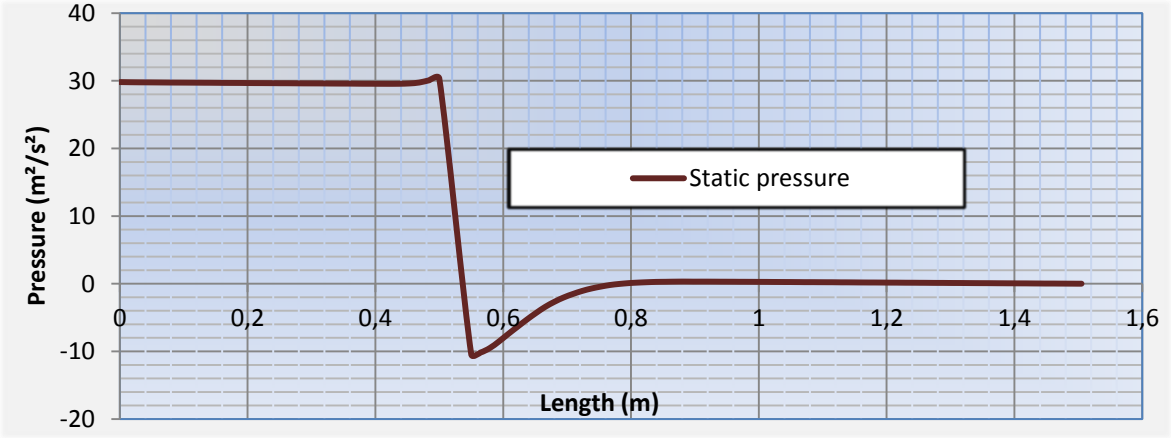

Figure 5: Static pressure in the orifice plate.

It is noted in the graph of the Fig. 5 that there is a small pressure spike just upstream of the obstruction geometry. It can also be noted that there is an unrecoverable portion of the pressure after passing the obstruction, called permanent head loss.

Through simulation, we obtained the processed pressure loss, which allows the calculation of the discharge coefficient through Eq. 1. Therefore, it was extracted the value of the pressure drop between the point at a distance D upstream of the orifice and the point at a distance 0,5D downstream of the orifice, obtaining a numerical $C_d = 0,64$ for a pressure drop equivalent to 48,1 Pascal.

Using Eq. 2 is possible to find theoretical discharge coefficient because values of β, the Reynolds number and the correlation factors are known. So are obtained the analytical values of Cd = 0,62 and a pressure drop of 52,4 Pascal.

Therefore, it can be said that the physical structures acquired in the simulation are consistent with the physical structures presented in the literature, as well as the quantitative results attained show similarity which reaches almost

96% for the coefficient of discharge and 91% to the value of pressure drop, validating the numerical results of the simulations.

4.2 Prototype Results

After the experiments with the prototype on the bench flow and the realization of computer simulations, we obtained the results shown in Fig. 6.

Figure 6 shows the operation curve of the mixer, which relates the flow associated with the pressure differential between the extremes of the prototype.

It is noted that the values shown in the curve of operation of the numerical, analytical and experimental follow the same curve profile, although they have different absolute values. The profiles shown has a stronger inclination at low flow rates, indicating a tendency to be proportionally less pressure drop at higher flow rates. From another point of view, it can also be inferred that, proportionally, there is a lower pressure energy demand to induce higher flow rates or high Reynolds number flow.

With respect to the experimental values of Figure 6, the graphic illustrates its discrepancy in relation to numerical and theoretical results. This follows from a slight slack in fixing the flange on the flow bench, causing leakage. Thus, not all flow passed through the measuring bench, resulting in the effect of smaller experimental pressure loss.

It is noteworthy that for this specific case the analytical values calculated have associated errors. First, the discharge coefficient calculation shown in Eq. 2 takes into account the pressure measurements at a distance D upstream and 0,5 D downstream. However, these distances can't be observed due to the size of the prototype. Secondly, the geometry of the prototype tested does not allow full development of the region of recirculation and the recovery of the flow pressure, as showed in Fig. 7, factors considered essential in the development of theory equations 1 and 2 for analytical calculation results of load loss and coefficient discharge.

It is noted, despite this, that the correlation between the numerical and analytical values is reasonable, around 90%, and therefore the numerical results presented are deemed appropriate and characterize the physical situation of the real flow in the prototype tested.

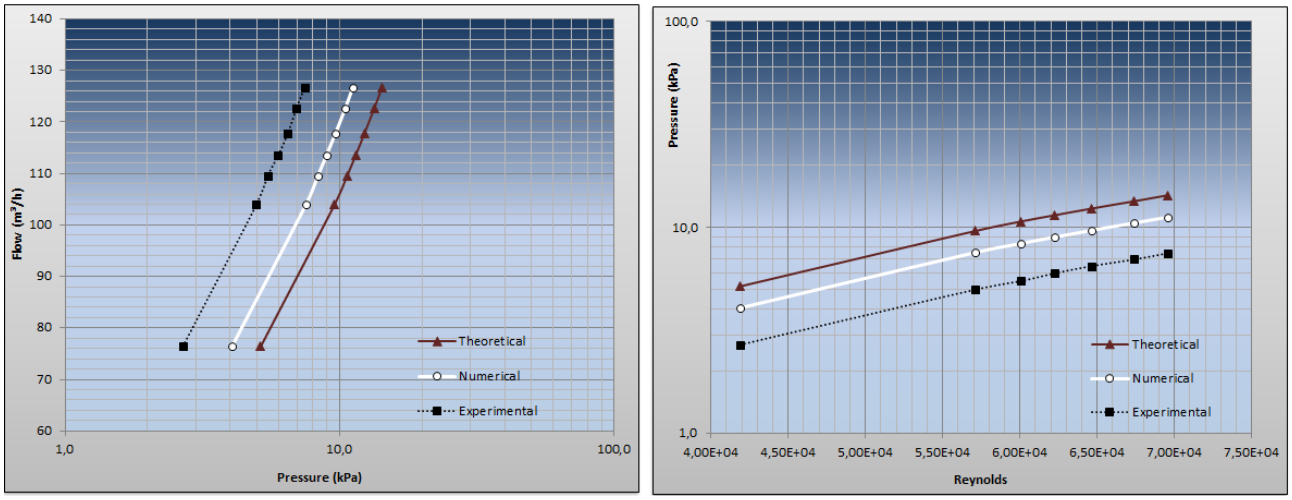

Figure 6: Operation curve of the mixer

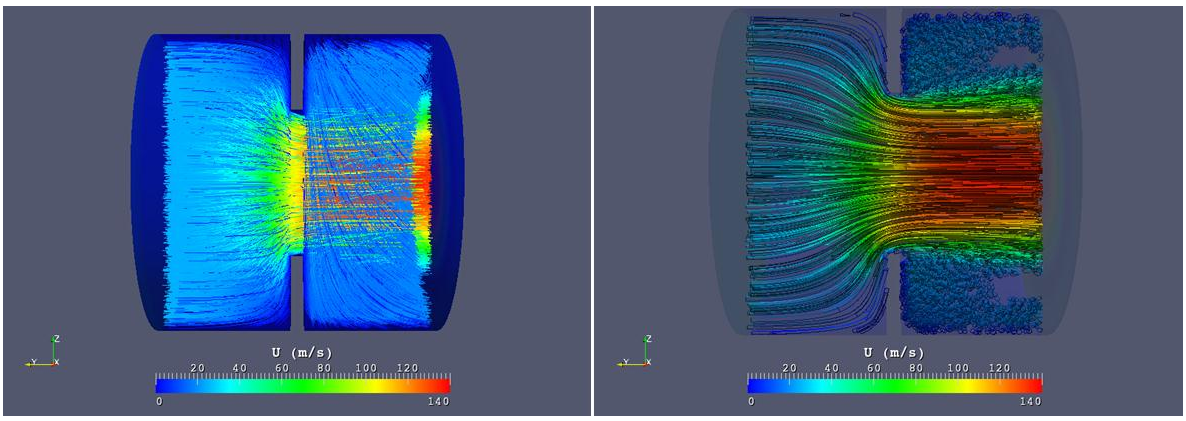

Figure 7: Region of recirculation of the flow in the prototype.

To evaluate the relationship between the mixing quality and the Reynolds number of the flow, we use the artifice of simulating the diffusion of a passive scalar in the flow. It is understood that the passive scalar diffusion through the turbulent convection flow can adequately characterize the mixing between natural gas and air. Figures 8, 9 and 10 illustrate the results obtained.

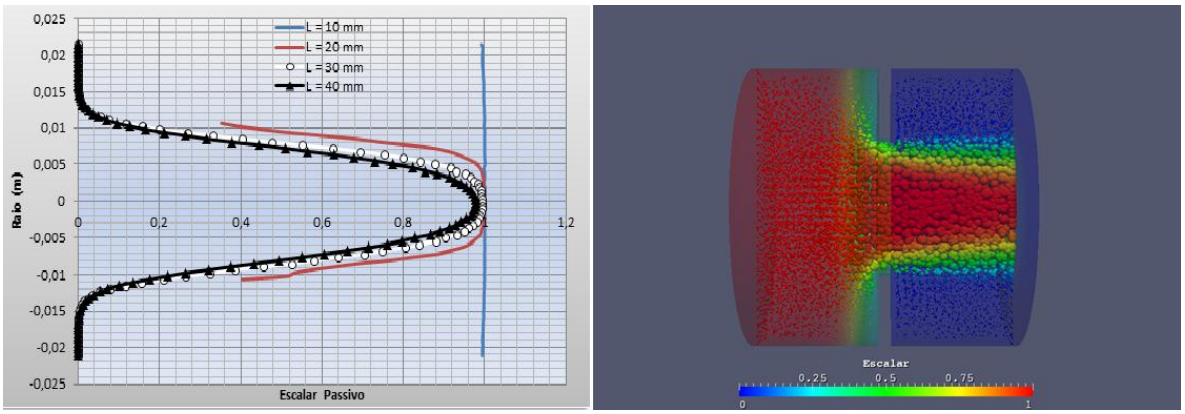

Figure 8: Diffusion of a passive scalar in the mixer with Reynolds number of 69000.

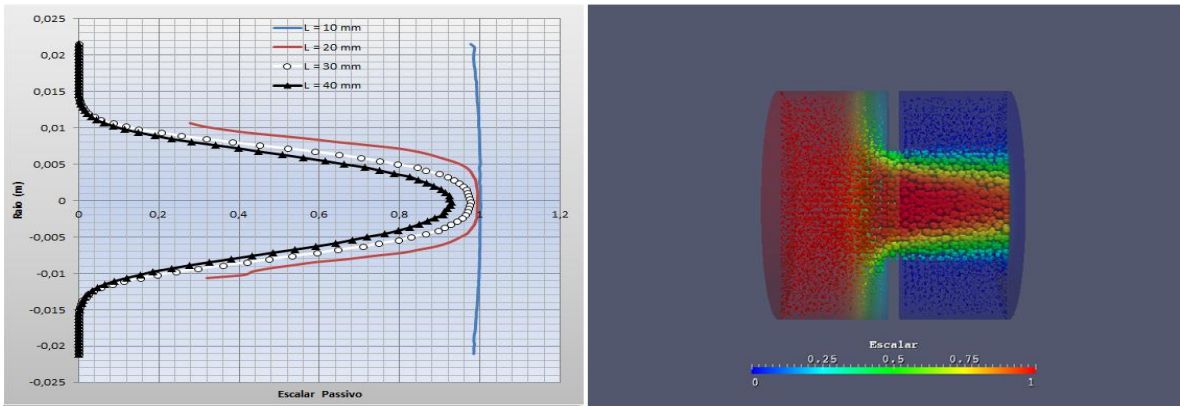

Figure 9: Diffusion of a passive scalar in the mixer with Reynolds number of 62000.

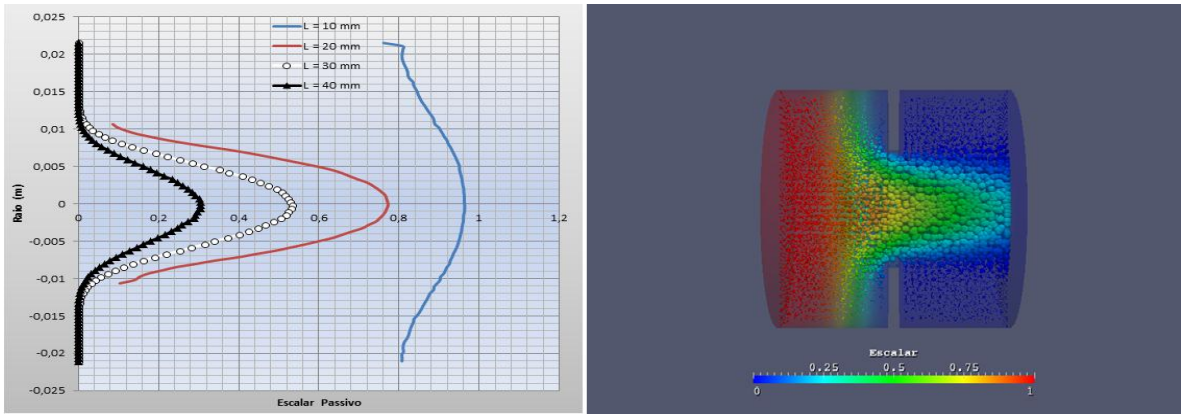

Figure 10: Diffusion of a passive scalar in the mixer with Reynolds number of 42000.

Firstly, it is observed that diffusion rate of the passive scalar is directly proportional to the Reynolds number of the flow. The graph of Figure 8 allows to observing that 10 millimeters from the entrance of the mixer the passive scalar occupies its whole circumferential region, while in Figure 10 at the same distance the circumferential distribution of the passive scale is uneven.

However, after the geometric constraint, it is clear that the influence of Reynolds number is practically zero with respect to the circumferential scalar passive diffusion. Figures 8-10 allow us to observe that at the output of the mixer the area occupied by passive scale is practically identical.

Approximately 10 millimeters from the centerline of the prototype there is no presence of the passive scale in the flow. This, in principle, indicates the trend that the mixture is not homogeneous because its characteristic is the presence of gas molecules across the circumferential region of the exit of the mixer.

Thus, the effect of recirculation flow in the low pressure zone after the geometric constraint is associated with a low rate of diffusion in this region.

As the flow of recirculation region has no geometrical conditions favorable for the recovery of the load and to return to the main flow, the geometry of the prototype tested influences in a dominant way the diffusion of molecules.

It is presumed therefore that a greater length of geometry tested allow an improvement of molecular diffusion, and consequently the homogeneity of mixing between gas and air at the exit of the mixer. In this sense, it also is observed that the shape of the geometric constraints imposed on the flow is a decisive factor in the quality of mixing, because it is exactly the step imposed to flow that generates the low pressure zone and hence the region of recirculation and low diffusion molecules in regions close to the walls at the exit of the mixer tested.

5. CONCLUSION

From the results obtained can be presented the following conclusions:

(i) The use of computer simulations is a reliable technique for the identification of characteristics and to predict profiles flow through orifice plates;

(ii) It appears that for the tested geometry exists a tendency to have a lower energy demand of pressure required to induce flow with Reynolds numbers greater. Through the graphs presented it is clear that variations in superior Reynolds number demand less variations of pressure energy. Thus, although the pressure drop is proportional to the Reynolds number of the flow, there appears to be a Reynolds number that serves as a point of stabilization of pressure loss. If this thesis is confirmed, it would mean that there would be a point at which the increased flow of air admitted through mixer would not lead to an increase in pressure loss;

(iii) It should be noted, though, that after the geometric constraint of the prototype tested the Reynolds number is not decisive factor that impacts the homogenization of the mixture. Moreover, the Reynolds number would be a major factor for the homogenization of the mixture should there be no restriction to the flow;

(iv) Finally, through the utilized methodology is concluded that the homogenization of the mixture after the geometric constraint of the mixer tested is a function of the geometrical shape of the prototype, which should be optimized through the search for alternative geometries; and that before to the geometric constraint the mixing quality is also a function of the Reynolds number of the not disturbed flow.

6. REFERENCES

Averous, J. e Fuentes, R., 1997, “Advances in the Numerical Simulation of Hydrocyclone Classification”, Canadian Metallurgical Quartely, v. 36, n. 5, p. 309-314.

Castro, J. A.. “Análise Comparativa da Qualidade da Mistura GNV-Ar em Misturadores com Geometrias Alternativas”. CONEMI 2008 - VIII Congresso Nacional de Engenharia Mecânica e Industrial.

Cullivan, J. C.; Williams, R. A.; Cross, C. R., 2003, “Understanding the Hydrocyclone Separator Through Computational Fluid Dynamics”, Trans IChemE, v. 81, p. 455-466.

Fox, R. W.; McDonald, A. T.; Introdução à Mecânica dos Fluidos, 5ª ed., Ed. LTC, Rio de Janeiro, 2001. Pg. 251.

Jones, W. and Launder, B.E., 1972, “The prediction of laminarization with a two equations model of turbulence”, International Journal os Heat and Mass Transfer, vol. 15,pp. 301-314.

Launder, B. E. e Spalding, D. B., 1972, “Lectures in Mathematical Models of Turbulence”, London: Academic Press, England.

Malhotra, A.; Branion, R. M. R.; Hauptmann, E. G., 1994, “Modelling the Flow in a Hydrocyclone”, Canadian J. Chem. Eng., v. 72, p. 953-960.

Mit, A. I. (2010).”The Future of natural Gas. Management”. Massachusetts Institute of Technology.

Munson,B.R, Young, D.F., Okiishi, T.H., 2002, “Fundamentals of fluid mechanics. 3 ed.

Patankar, S. V. e Spalding, D. B., 1972, "Calculation Procedure for Heat, Mass and Momentum Transfer in Three-Dimensional Parabolic Flows", Int. J. Heat Mass Transfer, v. 15, p. 1789.

White, F. M.; Mecânica dos Fluidos, 4ª edição, Ed. McGraw-Hill, Rio de Janeiro – RJ, 2002. Pg. 276/278.

7. RESPONSIBILITY NOTICE

The author(s) is (are) the only responsible for the printed material included in this paper.